Spectroscopy Letters

An International Journal for Rapid Communication

ISSN: 0038-7010 (Print) 1532-2289 (Online) Journal homepage: http://www.tandfonline.com/loi/lstl20

Mid-infrared carbon dioxide sensor with wireless and anti-condensation capability for use in greenhouses

J. N. Wang, Q. S. Xue, G. Y. Lin & Q. J. Ma

To cite this article: J. N. Wang, Q. S. Xue, G. Y. Lin & Q. J. Ma (2018): Mid-infrared carbon dioxide sensor with wireless and anti-condensation capability for use in greenhouses, Spectroscopy Letters, DOI: 10.1080/00387010.2018.1468785

To link to this article: https://doi.org/10.1080/00387010.2018.1468785

Published online: 03 Jul 2018.

SPECTROSCOPY LETTERS
https://doi.org/10.1080/00387010.2018.1468785

Taylor & Francis
Taylor & Francis Group

Mid-infrared carbon dioxide sensor with wireless and anti-condensation capability for use in greenhouses

J. N. Wang, Q. S. Xue, G. Y. Lin and Q. J. Ma

Changchun Institute of Optics, Fine Mechanics and Physics, Chinese Academy of Sciences, Changchun, China

ABSTRACT

A mid-infrared carbon dioxide sensor with wireless and anti-condensation capability was experimentally demonstrated for greenhouse application. The sensor included an optical module integrated in a multi-pass gas chamber using the dual-channel detection method to suppress environmental noise. Considering the condensation phenomenon in the greenhouse, the optical chamber was protected with a breathable waterproof coverage. The field test demonstrated that the internal optical framework was kept in stable relative humidity, ensuring the sensor's applicability in the greenhouse. For wireless communication, received signal strength indication was used to ensure the reliability of link quality and enable smart power regulation. In related experiments, there was a satisfying performance in terms of stability and error detection within the measurement range of 30 – 5000 ppm. Without increasing the integral time, the limit of detection of the sensor was at least 30 ppm, which was acceptable for greenhouse application. A field test was carried out in Town Shelin of Jilin Province, China and the test showed the proposed sensor had relatively good prospect for application in fine agriculture.

ARTICLE HISTORY
Received 14 December 2017
Accepted 20 April 2018

KEYWORDS
carbon dioxide sensor; condensation; infrared absorption; orthogonal locked amplifier

Introduction

With the deep investigation of precision agricultures, the integration of traditional agricultural and electronic technology has been a desired research direction and is flourishing in Chinese agriculture.[1–3] The crop yield from solar greenhouse has increased by more than 3400 km^2 from 1820 to 2010.[4] Agriculture within greenhouses is still labor-intensive compared to other industries which is obviously lacking information technology application. Because of significant effect of crop yield increase and relative development of greenhouse farm, vertical farming with monitoring and management system gradually takes the place of the traditional agricultural in greenhouse.[5,6]

The environmental factors including temperature, humidity, and luminance and carbon dioxide concentration have a combined effect on the crop yield and health state of plants. However, in view of fine greenhouse application, the related research on cost performance, applicability to complex conditions and desired detection performance of carbon dioxide sensor is still insufficient.[7,8]

Existing carbon dioxide sensing techniques normally includes semiconductor, electrochemical, and infrared absorption spectroscopy.[9–11] However, the mixed gases which are used for producing crops, insects and fertilizers, limit the application of semiconductors sensors in special environment of greenhouse. Therefore, the general utilized sensor in greenhouse is electrochemical sensor, such as MG811, which requires long warm-up time, high temperatures working conditions, and large amount of energy consumption. Besides the harsh working conditions, the low measurement limitation of electrochemical sensors like MG811 is nearly 400 ppm which cannot satisfy the special requirement of greenhouse which usual has a closed configuration and at least lower than 200 ppm carbon dioxide concentration at noon. In contrast, the infrared absorption spectroscopy technology is able to satisfy kinds of various desires like measurement accuracy, high sensitivity, long time stability, and wide measurement range.

In the selection of infrared absorption technologies in the application of agriculture, photo-acoustic spectroscopy (PAS) detector has a desired sensitivity having an advantage on trace gas detection. But the capability in complex environment is insufficient.[12] The shortage of tunable diode laser absorption spectroscopy (TDLAS) technology in the field of agriculture is an exorbitant economic cost.[12,13] The current researches extend the application of tunable diode laser to carbon dioxide detection in agriculture.[14] However, the relative weak absorption in near infrared region have to rely on longer integration time (2.5 min) to improve the low limitation of detection which is not able to satisfy the real-time detection request.

In consideration of the cost-effective, special application environmental conditions and practical accuracy requirement of agriculture, the direct absorption spectroscopy (DAS)[15,16] technology was more favored compared with other relative technologies. Carbon dioxide sensor based on DAS using light-emitting diode (LED) and thermal light

CONTACT Q. J. Ma 243532757@qq.com Changchun Institute of Optics, Fine Mechanics and Physics, Chinese Academy of Sciences, Changchun 130033, China.
Color versions of one or more of the figures in the article can be found online at www.tandfonline.com/lstl.
Supplemental data for this article can be accessed here.

source have been developed and even produced in mass production. As a light source, LED is able to be modulated by a high frequency and has a high stability in long time working. However, the weak infrared emission power limits the detection performance.[17] The commercial sensors using thermal light source, such as K30, normally have a high integration with low cost.[18] As the price of high integration structure, a short absorption path with signal channel limits the detection performance and repeatability. As an application experience, commercial sensors are recommended to be calibrated every two or three months. Low sampling frequency limits the future gas fertilization performance. In addition, the capability in high humidity environment and real-time state monitoring of sensor are the common defects of commercial sensors. In order to make up the disadvantages mentioned above, a self-developed sensor with gas chamber with spherical mirror and anti-condensation protection was designed and fabricated to increase optical path and ensure the capability in greenhouse. Differential detection technology with 4 Hz modulation is used to avoid the effect from light source aging and dust accumulation.

Besides the related carbon dioxide sensing technologies, the common term wireless sensor network (WSN) widely used in regional surveillance and monitoring application is adopted to equip sensor nodes with wireless data transmission ability and form a data collection network for information acquired from each sensor nodes.[1,19,20] In the utilizations of WSN in greenhouse, the received signal strength indication (RSSI) is a common method to evaluate the valid communication distance between the sensor nodes and terminals.[21]

In consideration of the special environmental influences of greenhouse, the condensation occurs on the surface of optical module is urgent to solve. In the term of the optical module of sensor using NDIR technologies, dew condensation would cause serious errors from light absorption, scattering, refraction, and reflections. In addition, the temperature difference caused by the semi closed structure of sensor provides an advantaged condition for dew condensation. A prevention system for forecasting the dew condensation based on dew condensation temperature calculation[22] is designed and fabricated with the real-time environmental information measurement.

Sensor node design

Sensor node configuration and theory

According to application requirements in solar greenhouse, an infrared carbon dioxide sensor was designed and fabricated aiming to satisfy the specific measurement requirements. Fig. 1 shows the schematic diagram of the carbon dioxide sensor node, including the optical and electrical parts. In the optical part, the light source and detector were integrated in a chamber with a spherical reflector to increase the transmission length. Infrared light from a wideband infrared source (IR55) was reflected by the spherical reflector and was received by a dual–channel Pyroelectric detector (LM244). In electrical part, both differential signals and light source driving current were processed and generated by the

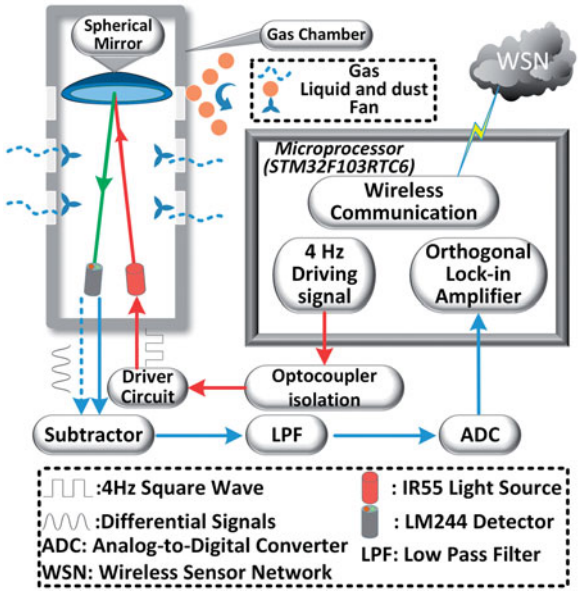

Figure 1. Structure of the mid-infrared carbon dioxide sensor node. Detail of sensor structure including a spherical reflector was used to optimize the optical path, condensation protection covering the chamber surface, driving, and signal processing circuits are shown.

micro-controller (STM32F103RTC6). The original voltage signals measured from detector were processed by the integrated pre-amplification (PA), subtractor, low pass filter (LPF), and an analog-to-digital converter (ADC). The measured data were processed as digital signals by a self-developed orthogonal lock-in amplifier.

For sensor protection during application in complex environments like a greenhouse, the optical part was protected by a waterproof breathable coverage. Environmental parameters, including temperatures and humidity of air, the sensor, and leaves were also measured. Besides the above mentioned components, a 433 MHz wireless communication module was integrated with the sensor to realize a closed loop feedback through wireless data transmission between a laptop terminal and sensor nodes.

Considering actual request in fine agriculture, a low cost infrared light source (IR55) with a wide spectrum covering the measurement wavelength was selected for the carbon dioxide sensor. The detector received two central wavelengths with two filter windows at 4.26 μm and 4.00 μm, respectively, corresponding to the absorption and non-absorption regions of carbon dioxide, respectively. The relationship between the desired carbon dioxide concentration and received voltage signals could be calculated based on the Beer-Lambert law, as shown in Eq. [1]:

$$I = I_0 \exp(-KCL) \tag{1}$$

Where I is the light signal received by the two filtering windows, I_0 is the initial emission light signal power, K is the absorption coefficient, C is carbon dioxide concentration, and L is the optical length (30 cm). Defining k_1 and k_2 as the optical-to-electrical conversion coefficients at λ_1 and λ_2, respectively, the amplitudes U_1 and U_2 of detection signals are derived shown in Eqs. [2] and [3]:

$$U_1 = I_0 k_1 \exp(-KCL) \tag{2}$$

$$U_2 = I_0 k_2 \tag{3}$$

With $\Delta U = U_2 - U_1$ and based on the above equations, carbon dioxide concentration can be determined using Eq. [4]:

$$C = \frac{1}{KL} \ln\left[\frac{k_1}{k_2}\left(1 - \frac{\Delta U}{U_2}\right)\right] \tag{4}$$

Indeed, under practical circumstances, the influences of scattering, Raleigh scattering, Mie scattering and water vapor absorption should be calculated theoretically. However, considering that the two filter peak wavelengths $\lambda_1 = 4.26\,\mu m$ and $\lambda_2 = 4.00\,\mu m$ are extremely close to each other, the influential coefficients are small enough to be neglected compared with other influential factors such as environmental noises. Under inherent characteristics of the differential detector, the scattering and absorption coefficients could be eliminated through calculation. Besides in the above analysis, Eq. (4) was used to define the relationship between carbon dioxide concentration and measured voltage signals, which were demonstrated through calibration experiments.

Light source and detector selection

According to the high-resolution transmission molecular absorption database 2004 or HITRAN 2004, the absorption spectrum of carbon dioxide was plotted in Fig. 2, including the absorption and reference wavelengths around 4.26 μm and 4.00 μm, respectively. Taking into consideration the greenhouse application conditions, methane, and water have a relative high concentration and more attention should be paid. In addition, other possible components with low concentration, such sulfur dioxide, are at least five orders of absorption magnitude lower than carbon dioxide and their effects were ignored. To eliminate the potential interference of water and methane, the absorption spectra of water and methane around the absorption and reference ranges are shown in the figures as well. As shown in Fig. 2a, absorbance values of water and methane were nearly five orders of magnitude lower than that of carbon dioxide around 4.26 μm. In addition, Fig. 2b shows almost no absorption near 4 μm for carbon dioxide, water, and methane. Hence, 4.26 μm and 4.00 μm were used as detection channel and reference channel. Based on the analysis of the above absorption and reference spectra, a Perkin Elmer's dual–channel pyroelectric detector with a detectivity (D^*) of 3.5×10^8 cm $Hz^{1/2}/W$, equipped with the responding filter windows at 4.26 μm and 4.00 μm, was selected as detector of this sensor. The original voltage difference, which was lower than 10 mV, was amplified by the inherent pre-amplifier to simplify the following signal processing.

According to the spectral range of the selected detector and cost-effectiveness requirements, an infrared light source (IR55) fabricated with the micro-electromechanical system (MEMS) technology was used as the light source, with a wide emission spectrum range covering both the absorption and reference ranges. Based on the response curve of both the detector and light source, the modulation frequency was limited to under 10Hz. In the range below 10Hz, 4Hz modulation had the highest signal to noise ratio (SNR) and was selected as the modulation frequency.

In consideration of the thermal characteristic of light source, the stable time needed after startup is a critical parameter for practical application. After an experiment, the time for the temperature to enter the stable region was 51 second with a fluctuation less than 1° as shown in Fig. 3a. When the light source is under stable state, the spectrum of the driven IR55 is shown in Fig. 3b, covering a wide range of wavelengths, from near- to mid-infrared. The detailed emission spectrum corresponding to the two filter windows of the detector is shown in the inset of Fig. 3b. In practice, relatively high amounts of carbon dioxide originate from the operator and humidity in air corresponds to most absorption near 4.26 μm and 5.5-7.5 μm, respectively.

Development of a waterproof optical module

In order to enable the application of a sensor based on the non-dispersive infra-red (NDIR) technology in the greenhouse environment, the dew condensation phenomenon on optical

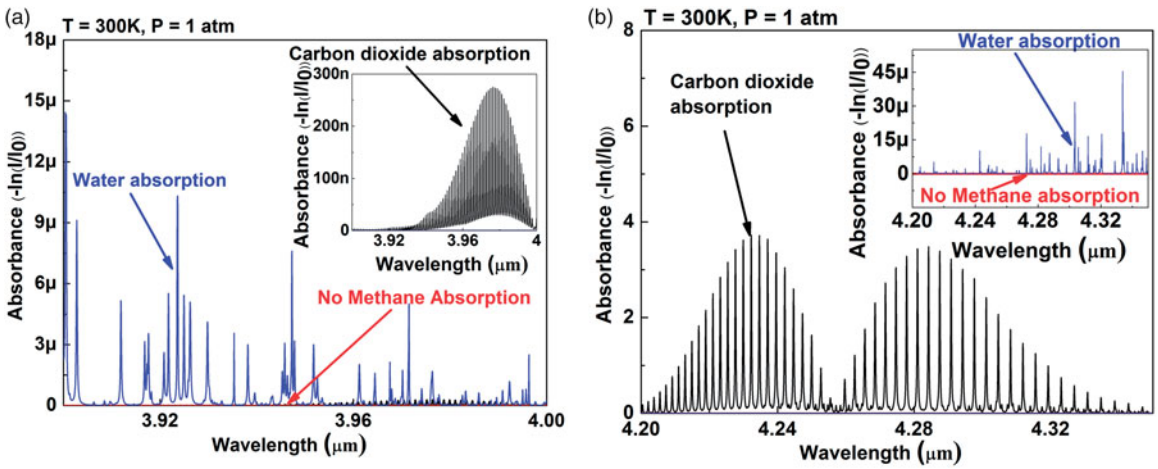

Figure 2. Spectra from the dual channel carbon dioxide sensor for greenhouse use. (a) Carbon dioxide absorption compared with water and methane in the detection channel ~4.26 μm; (b) Absorption spectra of water and methane compared with carbon dioxide in the reference channel ~4.0 μm.

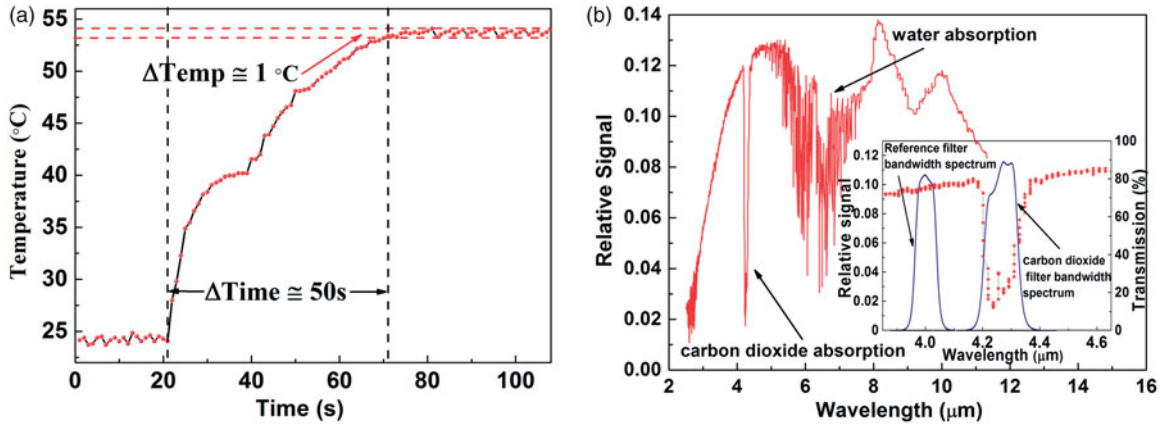

Figure 3. Emission spectra of IR55. (a) Preheat time experiment result; (b) The required spectra range is covered by the emission spectrum of IR55 and spectra respond the filter windows of detector at 4.26 μm and 4.0 μm are shown in insert.

components should be paid more attention to. In the greenhouse environment, dew condensation occurs when the temperature of the sensor's components is lower than the dew point. Besides air temperature and relative humidity, the components temperature in the optical part was also measured for real-time anti-condensation. In addition, current treatment options for diseases and insect pests are mainly based on early prevention and control. Considering the proliferation of diseases caused by dew formation on the leaf surface, the leaf temperature on a non-direct sunlight surface with lower temperature (i.e. easily affected by dew formation) was measured for warning and relative regulation.

For dew point calculation, the variable factors used were ambient temperature and humidity measured by the environmental sensor nodes as well as the temperature of components in the optical part. T_{dew} was defined as the dew condensation temperature. Based on a report by Barenbrug et al.[23] for dew point calculation, with the parameters a and b having constant values, the dew condensation temperature was calculated by using Eqs. [5] and [6] with an error of ±0.4 °C.

$$T_{dew} = \frac{b \times \alpha(T, RH)}{a - \alpha(T, RH)} \tag{5}$$

$$\alpha(T, RH) = \frac{a \times T}{b + T} + \ln(RH/100) \tag{6}$$

In the above equation, the relevant parameters T and RH are temperature in degrees Celsius and relative humidity, respectively. With the dynamic changing of temperature or humidity, the dew condensation temperature may be close to or even above the surface temperature of plants, indicating condensation occurrence.

Besides a compromised selection between waterproof ability and breathability, the capability to sustain high humidity and temperature should also be considered. Therefore, breathable waterproof membranes made of expanded polytetrafluoroethylene (ePTFE) were selected and used to cover ventilation holes. The permeability of ePTFE was higher than 480 ml/min, with superior performance compared with commonly used materials like thermoplastic polyurethanes (TPU). Moreover, the chemical stability of ePTFE could protect the sensor from corrosion caused by fertilizers. Finally, considering the high surface temperature of the sensor caused by prolonged direct sunlight, the anti-high-temperature ability of ePTFE (up to 250 °C) is also able to satisfy this requirement. The selected breathable waterproof membranes were placed on vents close to fans to enable adjustable gas flow velocity between the optical parts and outside.

Digital lock-in amplifier

In this detection system, a digital lock-in amplifier was developed. The two inputs of the digital orthogonal lock-in amplifier were differential and 4 Hz square reference signals, respectively. Irradiated with the modulated light, the detector generated two signals, and the differential signal was obtained through a differential amplifier. The reference signal was generated by the driving 4 Hz square signal to replace the sine wave, which is able to suppress the quantization error.

After the sampling, the phase of the reference signal was shifted by 90°. The two output voltage signals were processed by two low pass filters. The amplitude of the absorption amplitude signal could be calculated with a high signal and noise ratio.

Wireless communication

To avoid the difficulty of wire installation, Si4463, a highly integrated wireless industrial scientific medical band transceiver chip working in 433 MHz, was integrated to the electrical part of the sensor. Compared with traditional wireless modules, Si4463 has extremely low receiver sensitivity (−126 dBm), even lower in the actual experiment, and an adjustable output power of up to +20 dBm, effectively enhancing the transmission region and improving the link communication performance.

In the communication process, besides sensor identification, the collected environmental data and acknowledgement signal, the real-time RSSI value was also packaged in accordance with the communication protocol. The RSSI value was measured following the receiver transmitted data to evaluate the quality of the wireless communication signal, which reflected the situation of the communication environment. In

different plant growth phases, the sensor node is able to adjust the transmission power according to the real-time RSSI value obtained with the shielding effect of plants. Considering the balance between energy consumption and the data loss rate, the default feasible RSSI range was set from −75 dBm to −90 dBm, which can be adjusted based on special requirements. The selective transmission power from 0 dBm to 20 dBm with a 3 dBm one step would be adjusted automatically when the actual measured RSSI value is out of the feasibility range.

For the field test, the sensor node was installed at a height of 1.2 m and the communication was reliable within 85 m (RSSI is −90 dBm at 85 m) under a 20 dBm transmission power. With a transmission distance longer than 110 m (loss rate less than 1% within 110 m), the data loss rate showed a relatively dramatic increase.

Comparison with commercial sensors

Based on the NDIR technology, small size commercial sensors have already been designed by Senseair Company (K30) and ELT Sensor Company (S300 and T100).[18,24] However, compared with the sensor developed in this work, the commercial sensors have several disadvantages as follows:

First, there was insufficient precision and stability (about 3% of reading ±50 ppm), not satisfying the measurement requirements of the related low detection range.

Secondly, according to gas experiments, at carbon dioxide concentration lower than 60 ppm, an inverse relationship existed between the measured and standard concentrations, which may mislead the future irrigation strategy. This experimental result is presumably caused by the common impact of the software algorithm embedded in the commercial sensor and insufficient level of detail.

Thirdly, compared with the two-channel differential detection method used in the designed sensor, commercial sensors with single-channel detector do not guarantee long term repeatability and stability. Indeed, remedial correction is recommended every two or three months.

Finally, considering the future control of carbon dioxide concentration, the typical sample period of commercial sensors is 3 s, which significantly limits control's precision.

The humidity range of application of the self-made CO_2 sensor is separately considered by two parts. The inside part of sensor is protected by a waterproof breathable cover and the humidity is kept relatively constant. The applicable range of outsider part including temperature sensor and wireless mode is up to 95% according to the datasheet. Therefore, the final humidity range is set to 0–95%.

According to a temperature experiment, the temperature range of application of the self-made CO_2 sensor is 0 to 50 °C. In addition, when the temperature is higher than 50°, there is an error caused by the increased temperature on the light source.

Sum up, the range of application of the self-developed NDIR sensor is 0–95% and 0–50 °C.

Experiment and calibration

Gas preparation and noise analysis

During the experiment and calibration, to avoid operation errors caused by the external pressure difference, dynamic gas distribution was used instead of static injection distribution. During the experiment, the gas sample was continuously pumped into the chamber with a certain gas flow. An exhaust pipe was installed on the other side of the chamber to eliminate excess gas and maintain constant pressure. Because the possible impact caused by interference gases, such as water and methane, has been filtered out theoretically as described in the sections "Light source and detector selection and Development of a waterproof optical module," the gas samples only includes carbon dioxide and nitrogen (N_2). In fact, according to the field test, the methane concentration is about 120 ppm and the ammonia and sulfur dioxide concentration is low enough to be ignored. To ensure result accuracy, the gas samples used for gas distribution were 5000 ppm carbon dioxide with 2% uncertainty and 99.999% pure N_2. The different concentrations of gas-carbon dioxide required were obtained by mixing the two standard gas samples mentioned above through a mass flow meter (MT50-3G). In noise assessment experiments, the chamber was continuously flushed with pure N_2 to maintain a zero carbon dioxide concentration in the environment.

A high SNR is a desired parameter in sensor design, reflecting the sensor's performance including accuracy and the detection limit. In the SNR experiment, both the noise characteristics sampled after pre-amplifier of the sensor under turn-on state and turn-off state of the light source were measured using a radio-frequency spectrum analyzer. Under the turn-off state, the noise at modulation frequency (4 Hz) is lower than −70 dBm in both detection and reference channels. Under the turn-on state, the bandwidth of 10 dB at 4 Hz was nearly 1.6 Hz indicating the desired performance and high SNR of this sensor.

Calibration experiment

In the calibration experiment, a series of required gas samples, from 0 ppm to 5000 ppm were distributed and flushed into the chamber. Until sufficient stability the measured data ΔU was recorded over more than 10 min for each concentration. The fitting curves between average ΔU and the carbon dioxide concentration C, and the related fitting equation are shown in Fig. 4. The desired carbon dioxide concentration was obtained using Eq. [7]:

$$C = 43.3 - 1774.38 \times \ln\left(\frac{0.2001 - \Delta U}{1.3428}\right) \tag{7}$$

To verify the accuracy of the fitting, different gas samples were distributed from 0 ppm to 5000 ppm and the developed sensor was employed to measure the concentration of each gas sample. The concentration of the prepared gas sample was treated as the standard concentration and named X, while the concentration reading from the sensor was termed Y. The slope indicating the relationship between the measured and standard carbon dioxide concentrations was very

close to one with an ignorable offset, which demonstrated a high accordance between measured and standard values. When the measured carbon dioxide concentration was higher than 50 ppm, a relative detection error below 3.7% was obtained. In the low concentration range from 15 ppm to 50 ppm, a relatively longer integral time and average calculation is recommended to achieve the desired measurement performance according to the specific requirements. For even lower concentration detection, the measurement performance cannot be guaranteed.

To measure the lower limit of detection, the chamber was first flushed with pure N_2. Then, the carbon dioxide mass flow was increased stepwise by 10 ppm. The measurement results are shown in Fig. 5a, without processing by any software algorithm. The lower limit of detection for the developed sensor was at least 30 ppm and even lower after optimization. Considering the carbon dioxide concentration in the atmosphere and the limited sealing performance in the greenhouse environment, this lower limit of detection is acceptable for greenhouse application. Fig. 5b shows the Allan variance of the developed sensor, indicating its stability and the theoretical detection limit of the system. Long-term measurement was carried out under 0 ppm carbon dioxide. With integration time increased to 30 s, the influence from white noise was negligible where the slope differed from −1. With integration time increased to the intersection point of 0.5 slope, the detection system reached its theoretical detection limit of 15 ppm. At the cost of response time, the detection limit could be decreased, providing some flexible options for different application environments.

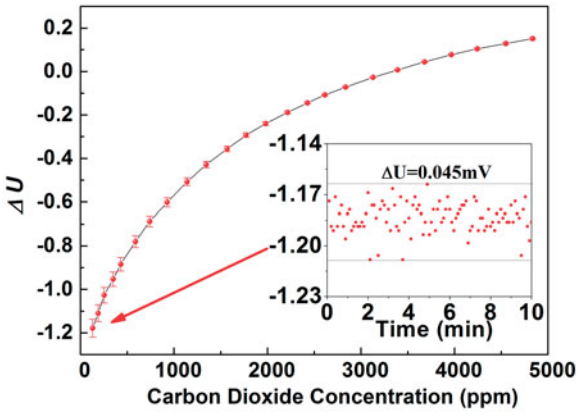

Figure 4. Relationship between measured voltage signal and carbon dioxide concentration. Dot plots and fitting curves for the measured differential value ΔU with carbon dioxide concentration C. At every concentration, 10 min samples were recorded (inset).

Detection stability

In the current experiments, gas samples were distributed and continually flushed into the chamber with a slow speed to simulate the practical situation of the greenhouse. Several gas samples with different concentration are prepared. As an example, 72 h results are shown in Fig. 6. Because of the combination influence of operation error, distribution error from mass flow and detection error of sensor, the fluctuations are 5.2%, 4%, 2.2%, 1.08%, and 0.5% at 100 ppm, 500 ppm, 1000 ppm, 2000 ppm, and 4000 ppm, respectively. During the long-term test, there is no measurement drift and spikes occurrence which indicates a desired detection stability.

Field test results and discussion

Environmental factors in the field test results

To test the application performance of the designed sensor, field tests were carried out in Town Shelin in Jilin Province. Several self-developed sensors are deployed in greenhouse and the most measurement data complied with the

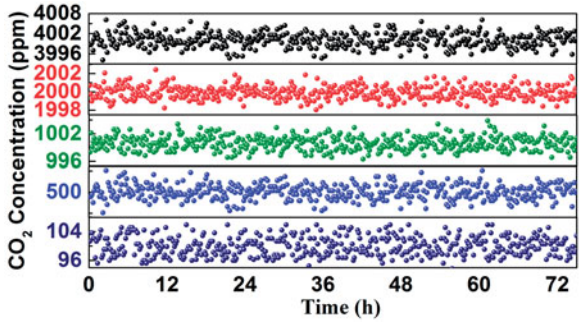

Figure 6. Stability data. Long-term measurement results from the five carbon dioxide standard samples at concentrations of 100 ppm, 500 ppm, 1000 ppm, 2000 ppm, and 4000 ppm, respectively for stability evaluation.

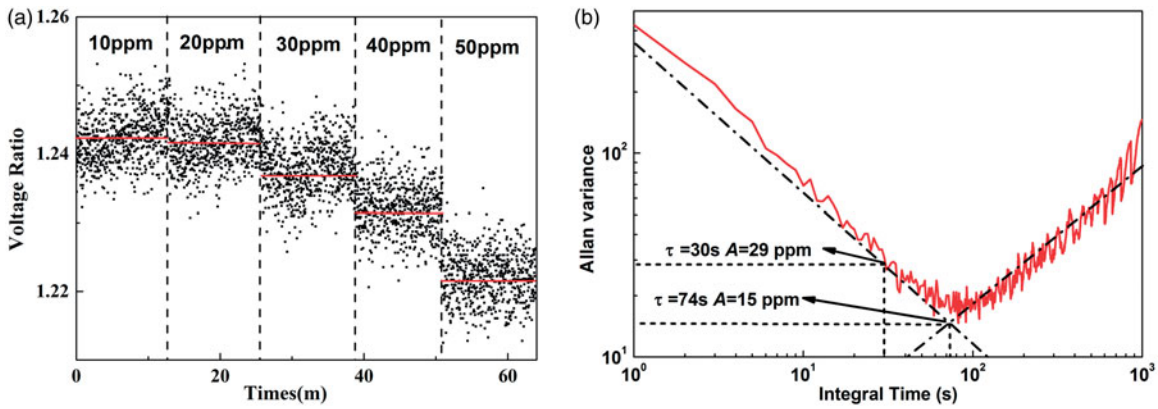

Figure 5. Low detection limit. (a) 50 ppm to 10 ppm carbon dioxide samples with 10 ppm stepwise increase were used in the experiment; (b) Allan's variance analysis.

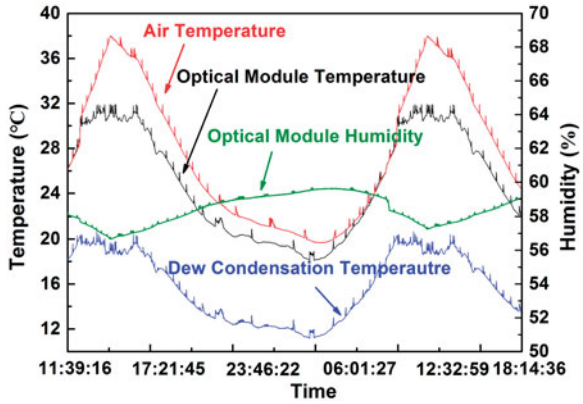

Figure 7. Field test for anti-condensation performance of the sensor. The real-time dew condensation temperature was calculated to indicate condensation risk.

photosynthesis law, indicating that the desired detection performance was achieved. Because of photosynthesis caused by strong luminance, the lowest carbon dioxide concentration in the greenhouse was below 280 ppm at about 13:00. At about the same time, the temperature of the greenhouse was increased to the peak about 35° with the lowest relative humidity about 78%. However, an unnatural phenomenon of luminance drastically decreasing to zero at 17:45 was observed. This might be because the greenhouse was covered with a ceiling driven by rolling machines for insulation, as frequently found in cold regions. In addition, a reasonable compensation of carbon dioxide gas fertilization corresponding to the plant species and growth stages is a potential application based on the proposed sensor system.

Anti-condensation field test results

According to the condensation phenomenon caused by diurnal temperature, the breathable waterproof membranes could insulate the optical part from the surrounding high humidity environment and maintained a constant relative humidity inside the shell. To accelerate the gas diffusion speed, four fans were installed on the ventilation holes, and their speed could be regulated according to the specific requirements. The test results for dew condensation in the field are shown in Fig. 7.

The black and red curves are the measured air humidity and internal humidity of the sensor, respectively. The internal temperature had a relatively smooth change trend compared with the outside air temperature, which is a useful method for preventing condensation. With the protection of breathable waterproof membranes made of ePTFE, the green curve representing internal humidity was maintained at a relatively low level. It is worth mentioning that the measured practical internal humidity of the sensor was not an ideal constant value but varied inversely with the environmental temperature in a small range (56% to 59%) due to complex environmental factors. The calculated dew condensation temperature in the optical part of the sensor was represented by the blue curve using the Barenbrug formula. Overall, during the whole day time, there were more than six temperature buffer ranges between the internal temperature and dew condensation temperature, indicating that the installed breathable waterproof membranes had effectively prevented condensation in the optical part of the sensor.

Conclusion

A differential mid-infrared carbon dioxide sensor with wireless and anti-condensation properties was designed and implemented. Compared with related researches and commercial sensors, a signal-source dual-channel detection system integrated into a chamber with anti-condensation protection effectively improves the detection accuracy, repeatability, and applicability in high humidity environment. The related experiments characterizes at least a 30 ppm lower limit of detection. Based on 72 h long-term stability detection on 100 ppm, 500 ppm, 1000 ppm, 2000 ppm, and 4000 ppm, the maximum detection errors are 5.2%, 4%, 2.2%, 1.08%, and 0.5% respectively. A field experiment was carried out and demonstrated that the self-produced carbon dioxide sensor could satisfy application requirements in the greenhouse. Besides its low cost, satisfactory precision, and robust performance, the sensor has a relatively high prospect in fine agriculture application.

Conflict of interest

No potential conflict of interest was reported by the authors.

Funding

This research was supported by the National Key Technology R&D Program of China (Nos. 2016YFB0500300, 2016YFB0500301, 2016YFB0500302, 2016YFB0500303 and 2016YFB0500304), the National Natural Science Foundation of China (No.41575023), and Science & Technology Development Project, Jilin Province (20170204019SF).

References

[1] Ojha, T.; Misra, S.; Raghuwanshi, N. S. Wireless Sensor Networks for Agriculture: The State-of-the-Art in Practice and Future Challenges. *Computers & Electronics in Agriculture* **2015**, *118*, 66–84.

[2] Ma, X.; Liu, S.; Li, Y.; Gao, Q. Z. Effectiveness of Gaseous Carbon Dioxide, Fertilizer Application in China's Greenhouses between 1982 and 2010. *Journal of CO_2 Utilization* **2015**, *11*, 63–66.

[3] Makeenkov, A.; Lapitskiy, I.; Somov, A.; Baranov, A. Flammable Gases and Vapors of Flammable Liquids: Monitoring with Infrared Sensor Node. *Sensors & Actuators B Chemical* **2015**, *209*, 1102–1107.

[4] Yap, F. G.; Yen, H. H. A Survey on Sensor Coverage and Visual Data Capturing/Processing/Transmission in Wireless Visual Sensor Networks. *Sensors (Basel)* **2014**, *14*, 3506–3527.

[5] Hart, J. K.; Martinez, K. Environmental Sensor Networks: A Revolution in the Earth System Science? *Earth Science Reviews* **2006**, *78*, 177–191.

[6] Hwang, J.; Shin, C.; Yoe, H. Study on an Agricultural Environment Monitoring Server System Using Wireless Sensor Networks. *Sensors* **2010**, *10*, 11189–11211.

[7] Malaver, A.; Motta, N.; Corke, P.; Gonzalez, F. Development and Integration of a Solar Powered Unmanned Aerial Vehicle and a Wireless Sensor Network to Monitor Greenhouse Gases. [J]. *Sensors* **2015**, *15*, 4072.

[8] Salker, A. V.; Choi, N.-J.; Kwak, J.-H.; Joo, B.-S.; Lee, D.-D. Thick Films of in, Bi and Pd Metal Oxides Impregnated in LaCoO3, Perovskite as Carbon Monoxide Sensor. *Sensors & Actuators B Chemical* **2005**, *106*, 461–467.

[9] Misra, S. C. K.; Mathur, P.; Srivastava, B. K. Vacuum-Deposited Nanocrystalline Polyaniline Thin Film Sensors for Detection of Carbon Monoxide. *Sensors & Actuators A Physical* **2004**, *114*, 30–35.

[10] Wu, R.-J.; Hu, C.-H.; Yeh, C.-T.; Su, P.-G. Nanogold on Powdered Cobalt Oxide for Carbon Monoxide Sensor. *Sensors & Actuators B Chemical* **2003**, *96*, 596–601.

[11] Thompson, A.; Northern, H.; Williams, B.; Hamilton, M.; Ewart, P. Simultaneous Detection of CO_2, and CO in Engine Exhaust Using Multi-Mode Absorption Spectroscopy, MUMAS. *Sensors & Actuators B Chemical* **2014**, *198*, 309–315.

[12] Pogány, A.; Ott, O.; Werhahn, O.; Ebert, V. Towards Traceability in Carbon Dioxide, Line Strength Measurements by TDLAS at 2.7 μm. *Journal of Quantitative Spectroscopy & Radiative Transfer* **2013**, *130*, 147–157.

[13] Li, G. L.; Sui, Y.; Dong, M. A Carbon Monoxide Detection Device Based on Mid-Infrared Absorption Spectroscopy at 4.6 μm. *Applied Physics B* **2015**, *119*, 287–296.

[14] Scholz, L.; Ortiz Perez, A.; Bierer, B.; Eaksen, P.; Wollenstein, J.; Palzer, S. Miniature Low-Cost Carbon Dioxide Sensor for Mobile Devices. *IEEE Sensors Journal* **2017**, *17*, 2889.

[15] Hodgkinson, J.; Tatam, R. P. Optical Gas Sensing: A Review. *Measurement Science and Technology* **2013**, *24*, 012004.

[16] Serôdio, C.; Boaventura Cunha, J.; Morais, R.; Couto, C.; Monteiro, J. A Networked Platform for Agricultural Management Systems.[J]. *Computers & Electronics in Agriculture* **2001**, *31*, 75–90.

[17] Bailey, D. M.; Adkins, E. M.; Miller, J. H. An Open-Path Tunable Diode Laser Absorption Spectrometer for Detection of Carbon Dioxide at the Bonanza Creek Long-Term Ecological Research Site near Fairbanks, Alaska. *Applied Physics B* **2017**, *123*, 245.

[18] Martin, C. R.; Zeng, N.; Karion, A.; Dickerson, R. R.; Ren, X.; Turpie, B. N.; Weber, K. J. Evaluation and Environmental Correction of Ambient CO_2 Measurements from a Low-Cost NDIR Sensor. *Atmospheric Measurement Techniques* **2017**, *10*, 2383–2395.

[19] Chen, T.; Su, G.; Yuan, H. In Situ Gas Filter Correlation: Photoacoustic CO Detection Method for Fire Warning. *Sensors & Actuators B Chemical* **2005**, *109*, 233–237.

[20] Garcia-Sanchez, A. J.; Garcia-Sanchez, F.; Garcia-Haro, J. Wireless Sensor Network Deployment for Integrating Video-Surveillance and Data-Monitoring in Precision Agriculture over Distributed Crops. *Computers & Electronics in Agriculture* **2011**, *75*, 288–303.

[21] Liu, H.; Meng, Z.; Cui, S. A. Wireless Sensor Network Prototype for Environmental Monitoring in Greenhouses[C]// International Conference on Wireless Communications. *NETWORKING and Mobile Computing. IEEE* **2007**, 2344–2347. doi:10.1109/WICOM.2007.584.

[22] Park, D.-H.; Park, J.-W. Wireless Sensor Network-Based Greenhouse Environment Monitoring and Automatic Control System for Dew Condensation Prevention. *Sensors* **2011**, *11*, 3640.

[23] Park, D. H.; Cho, S. E.; Park, J. W. The Realization of Greenhouse Monitoring and Auto Control System Using Wireless Sensor Network for Fungus Propagation Prevention in Leaf of Crop. *Control and Automation* **2009**, *65*, 28–34.

[24] Yasuda, T.; Yonemura, S.; Tani, A. Comparison of the Characteristics of Small Commercial NDIR CO_2 Sensor Models and Development of a Portable CO_2 Measurement Device [J]. *Sensors (Basel)* **2012**, *12*, 3641–3655.